

Gold Complexes with Dithiothiophene Ligands: A Metal Based on a Neutral Molecule

Dulce Belo,^[a] Helena Alves,^[a] Elsa Branco Lopes,^[a] Maria Teresa Duarte,^[b] Vasco Gama,^[a] Rui Teives Henriques,^[a, b] Manuel Almeida,^{*[a]} Aarón Pérez-Benítez,^[c] Concepció Rovira,^[c] and Jaume Veciana^[c]

Abstract: The gold complexes *n*-Bu₄N-[Au(α -tpdt)₂] (**5**), *n*-Bu₄N[Au(dtpdt)₂] (**4**) and *n*-Bu₄N[Au(tpdt)₂] (**6**) based on new dithiothiophene ligands (α -tpdt = 2,3-dihydro-5,6-thiophenedithiolate, dtpdt = 2,3-dihydro-5,6-thiophenedithiolate and tpdt = 3,4-thiophenedithiolate) have been prepared and characterised. These gold(III) complexes are diamagnetic, but they can be oxidised with iodine to the paramagnetic compounds [Au(α -tpdt)₂]

(**8**), [Au(dtpdt)₂] (**7**) and *n*-Bu₄N-[[Au(tpdt)₂]_{*n*-2}] (**9**), which were isolated as fine powders and which exhibit paramagnetic susceptibilities that are almost temperature independent with room temperature values of 2.5×10^{-4} , $2.0 \times$

10^{-4} and 5×10^{-4} emu mol⁻¹, respectively. Interestingly, the neutral complex [Au(α -tpdt)₂] (**8**) as a polycrystalline sample displays the properties of a metallic system with a room temperature electrical conductivity of 6 S cm⁻¹ and a thermoelectric power of 5.5 μ V K⁻¹; this is the first time that this metallic property has been observed in a molecular system based on a neutral species.

Keywords: conducting materials • coordination chemistry • gold • magnetic properties • S ligands

Introduction

Since the first discovery of metallic behaviour in the organic compound TTF-TCNQ, TTF-based donors have been widely used as building blocks for the preparation of molecular conducting and superconducting materials.^[1] Square-planar transition metal complexes with dithiolene ligands can be viewed as the inorganic analogues of TTF donors, in which the transition metal replaces the central C=C bond of TTF. The metal bis(dithiolene) complexes can exhibit several oxidation states and a diversity of coordination geometries.^[2] Most often, they act as anionic counterions (formal metal oxidation state III) in charge-transfer solids with a variety of donors. In

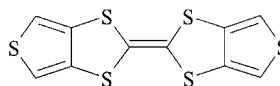
some cases, these metal complexes act as passive counterions that can be dia- or paramagnetic, depending on the metal,^[3] but in other cases, they are directly responsible for metallic^[4] or even superconducting properties^[5, 6] as in [Ni(dmit)₂] salts (dmit = 4,5-dimercapto-1,3-dithiole-2-dithione). Monoanionic gold bis(dithiolene) complexes can, in general, be reduced to paramagnetic dianionic species^[7, 8, 9] or, in some cases, can be oxidised to neutral radicaloid species.^[10, 11, 12] Higher oxidation states in gold and other transition metal bis(dithiolene) complexes have also been observed.^[13, 14]

In recent years, several new TTF-based donors have been reported which are fused with thiophene type rings, such as BET-TTF and DT-TTF, and were used with success in the

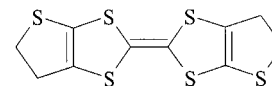
[a] M. Almeida, D. Belo, H. Alves, E. Branco Lopes, V. Gama, R. Teives Henriques
Instituto Tecnológico e Nuclear
Estrada Nacional n.º 10, 2686-953 Sacavém (Portugal)
Fax: (+351) 219941455
E-mail: malmeida@itn1.itn.pt

[b] M. T. Duarte, R. Teives Henriques
Instituto Superior Técnico
Av. Rovisco Pais, 1049-001 Lisboa (Portugal)
Fax: (+351) 218417862
E-mail: teresa.duarte@ist.utl.pt

[c] A. Pérez-Benítez, C. Rovira, J. Veciana
Institut de Ciència de Materials de Barcelona (CSIC)
Campus Universitari de Bellaterra, 08193 Cerdanyola (Spain)
Fax: (+34) 93-5805729
E-mail: cun@icmab.es



DTT-TTF



BET-TTF

preparation of different molecular conductors.^[15] In the charge transfer salts of these donors, the additional thiophene sulfur atom in the periphery of the donors allows extra intermolecular S...S contacts that control the crystal structure and the resulting electronic properties.

To the best of our knowledge, the transition metal bis(dithiothiophene) compounds, analogous to donors in

which the central C=C bond is replaced by a transition metal, have not been previously obtained. Herein we report the use of ketones **1** and **2** and thione **3**, precursors for the synthesis of thiophene substituted TTF donors,^[16, 17] in the preparation of the corresponding gold(III) complexes **4**, **5** and **6** (Scheme 1). Ketone **1**^[17] and thione **3**^[16] were previously known as precursors for the synthesis of the organic donors BET-TTF and DT-TTF, respectively. However, aromatised ketone **2** has not been previously reported. The oxidation of compounds **4**, **5** and **6** to the paramagnetic complexes **7**, **8** and **9**, and the study of all the compounds is also reported herein. The most interesting compound is complex **8**, since it shows an exceptionally large conductivity with metallic character; it is one of the very few conducting compounds based on neutral molecules, and the first that shows metallic transport properties (Scheme 1).

These gold complexes are the first members of an entirely new family of compounds based on dithiophene ligands with different transition metals. These will be reported in subsequent studies.

Results and Discussion

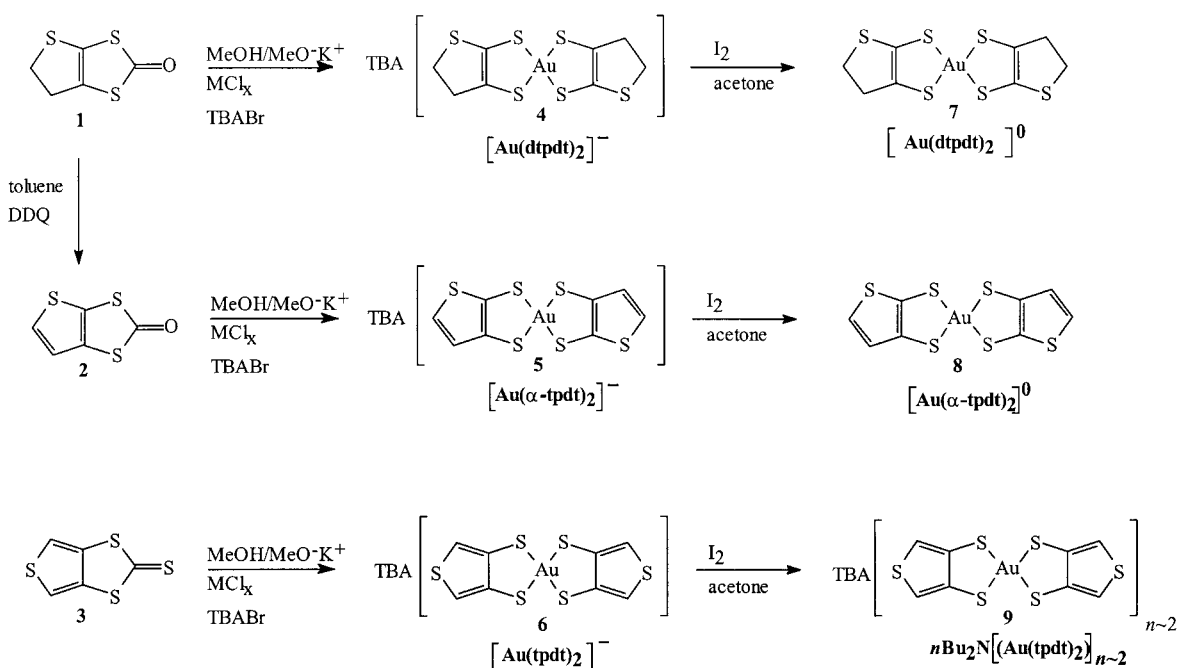
The syntheses of gold complexes **4**, **5** and **6** were performed following a general common procedure (Scheme 1). The thiophenedithiolate ligands were obtained in solution from the corresponding ketones **1**^[17] and **2** or thione **3**^[16] by hydrolytic cleavage with potassium methoxide in methanol. These ligands were treated immediately without intermediate isolation with potassium tetrachloroaurate to give the gold(III) complexes that precipitated as green-yellow (**4**), red (**5**), or brown-yellow (**6**) tetrabutylammonium salts after treatment with *n*-Bu₄NBr. The precipitates were washed with methanol and purified by recrystallisation in acetone/isopropyl alcohol

to give air-stable crystals. Final yields are in the range of 50–70%. Although not exhaustively tested, the same yields are obtained when either the ketones or the corresponding thiones are used. Elemental analysis results indicate a 1:1 stoichiometry for the *n*-Bu₄N salts of the gold(III) complexes as confirmed by X-ray crystal structure determination for complexes **4** and **6**.

Ketone **2** was obtained for the first time and in quantitative yield by aromatisation of **1** by refluxing with 2,3-dichloro-5,6-dicyano-1,4-benzoquinone (DDQ) in toluene.

Upon oxidation of the gold(III) complexes **4** and **5** with iodine, the corresponding neutral gold(IV) complexes [Au(dtpdt)₂] (**7**) and [Au(α-tpdt)₂] (**8**) were obtained as an almost insoluble dark fine powder. Due to the very low solubility of the neutral complexes in virtually all solvents tested, with exception of nitrobenzene in which it is only slightly soluble, it was not possible to grow single crystals for X-ray structure determination. In the case of *n*-Bu₄N-[Au(tpdt)₂] (**6**) only a partial oxidation by iodine was achieved as indicated by the elemental analysis obtained of the final product. Elemental analysis gave results that varied slightly from preparation to preparation, but were consistent with a stoichiometry close to *n*-Bu₄N[*n*-2] (**9**). The small deviations are ascribed to coprecipitation of impurities. This product is also very insoluble in all common solvents with the exception of nitrobenzene in which it is only slightly soluble.

The different oxidation behaviour of the gold bis(thiophenedithiolate) complexes is consistent with electrochemical studies. Cyclic voltammetry of *n*-Bu₄N[Au(α-tpdt)₂] in dichloromethane shows a pair of asymmetric redox waves, typical of the formation of an insoluble product, at (0.356, 0.556 V) 0.456 V versus Ag/AgCl that correspond to the couple [Au(α-tpdt)₂]⁻/[Au(α-tpdt)₂]. At lower potentials there is a pair of reversible waves centred at -1.162 V that



Scheme 1. Preparation of gold complexes **4**–**9**.

correspond to the couple $[\text{Au}(\alpha\text{-tpdt})_2]^{2-}/[\text{Au}(\alpha\text{-tpdt})_2]^-$. For $n\text{-Bu}_4\text{N}[\text{Au}(\text{tpdt})_2]$, the reversible waves that correspond to the $[\text{Au}(\text{tpdt})_2]^{2-}/[\text{Au}(\text{tpdt})_2]^-$ couple are observed at -0.900 V; at 0.754 V, a wave is observed whose peak intensity is approximately 50% of the previous one and which corresponds to a partial oxidation of the complex, possibly the couple $2[\text{Au}(\text{tpdt})_2]^-/[\text{Au}(\text{tpdt})_2]_2^-$. At higher potentials, a third irreversible wave is observed at 1.319 V and is ascribed to the full oxidation of the complex to the neutral species. For $[\text{Au}(\text{dtpdt})_2]$, the irreversible redox waves ascribed to the couple $[\text{Au}(\text{dtpdt})_2]^-/[\text{Au}(\text{dtpdt})_2]$ are observed at the lower values of $(0.122, 0.380 \text{ V})$ 0.201 V versus Ag/AgCl . This low oxidation potential is consistent with the observed instability of $n\text{-Bu}_4\text{N}[\text{Au}(\text{dtpdt})_2]$ solutions that slowly form a dark precipitate upon exposure to air.

Oxidation potentials of the studied complexes show an increasing facility to obtain the neutral species when the ligands are changed from tpdt to $\alpha\text{-tpdt}$ to dtpdt . Clearly the aromatic ligands $\alpha\text{-tpdt}$ and tpdt stabilise the anionic species. All of these complexes exhibit very low oxidation potentials when compared with more simple bis(dithiolene) complexes, such as $[\text{Au}(\text{mnt})_2]^{2-}$ ($\text{mnt} = 1,2\text{-dicyanoethylene-1,2-dithiolate}$) in which the neutral species is not as stable. The oxidation potentials of these dithiophene complexes from the monoanionic to the neutral species are comparable to those of other gold complexes with more extended aromatic ligands, such as $[\text{Au}(\text{bdt})_2]$ ($+0.86 \text{ V}$)^[12] and $[\text{Au}(\text{dddt})_2]$ ($+0.41 \text{ V}$)^[10] for which the neutral species were also isolated ($\text{bdt} = \text{benzo-1,2-dithiolate}$ and $\text{dddt} = 5,6\text{-dihydro-1,4-dithiin-2,3-dithiolate}$).

Despite the fact that well-formed single crystals were obtained for the tetrabutylammonium salts **4**, **5** and **6**, owing to severe twinning problems in the crystals of compound **5**, the crystal structure could be solved only for salts **4** and **6**.

In both complexes, the bond lengths in the thiophenic ring are close to those found in the corresponding TTF-based donors.^[16b, 18] The Au–S bond lengths observed in these complexes, with an average value of 2.319 \AA (see Table 1), are in the upper range of values reported for other gold(III) dithiolates^[15d, 19] that extend from 2.29 to 2.34 \AA with an average of 2.305 \AA .

By contrast, the $[\text{Au}(\text{dtpdt})_2]$ anion in **4** is significantly nonplanar and has only a *trans* configuration in the crystal (Figure 1), which is also the preferred configuration for the corresponding donor BET-TTF.^[16a, 17]

The nonplanarity of the $[\text{Au}(\text{dtpdt})_2]$ anion in **4** is denoted by the dihedral angle of 162.86° between the average plane of the two ligands. Additionally, there is a slight tetrahedral distortion of the four coordinating sulfur atoms that deviate by $\pm 0.14 \text{ \AA}$ from the average plane that contains the metal. These distortions are certainly due to the C–H \cdots S hydrogen bonds that are formed by all sulphur atoms except S(6) (see Table 2) and by the strong S(6) \cdots S(6)* interactions which twist the two ligands in opposite directions (see Figure 2 and the discussion of crystal packing below).

The $[\text{Au}(\text{tpdt})_2]$ anion in **6** is almost planar with a very small boat-type distortion (Figure 3). The gold atom and the four coordinating sulphur atoms S(1)–S(4) are coplanar within experimental error, with deviations smaller than 0.008 \AA . The

Table 1. Selected bond lengths [\AA] for compounds **4** and **6**.

	6	4
Au(1)–S(1)	2.315(5)	2.321(3)
Au(1)–S(2)	2.303(5)	2.319(2)
Au(1)–S(3)	2.305(5)	2.324(2)
Au(1)–S(4)	2.321(5)	2.321(3)
S(1)–C(1)	1.75(3)	1.76(1)
S(2)–C(2)	1.78(2)	1.73(1)
S(3)–C(3)	1.75(3)	1.74(1)
S(4)–C(4)	1.74(2)	1.74(1)
S(5)–C(5)	1.70(2)	
S(5)–C(6)	1.72(3)	1.78(2)
S(5)–C(2)		1.75(1)
S(6)–C(7)	1.74(2)	1.79(1)
S(6)–C(8)	1.71(3)	
S(6)–C(3)		1.776(9)
C(1)–C(2)	1.43(3)	1.33(1)
C(1)–C(5)	1.33(3)	1.58(1)
C(2)–C(6)	1.35(3)	
C(3)–C(4)	1.45(3)	1.32(1)
C(3)–C(7)	1.32(3)	
C(4)–C(8)	1.36(3)	1.62(1)
C(5)–C(6)		1.41(2)
C(7)–C(8)		1.49(2)

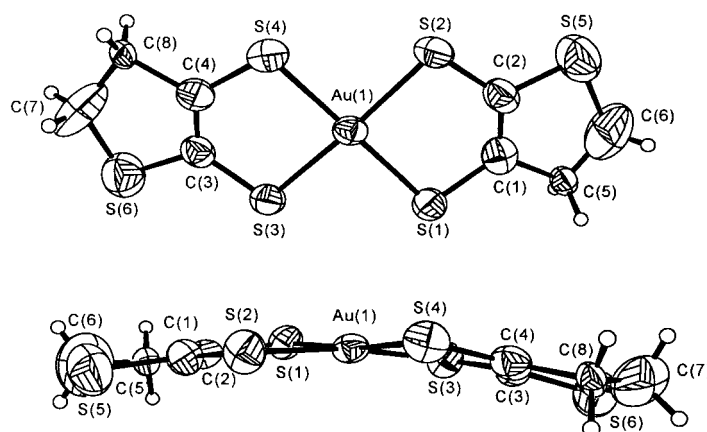


Figure 1. ORTEP views and atomic numbering scheme of $[\text{Au}(\text{dtpdt})_2]^-$ (**4**) with thermal ellipsoids at 40% probability level.

Table 2. Hydrogen bonds and short contacts in the crystal structure of compound **4**.

	d [\AA]	Angle [$^\circ$]
C(12)–H(12a) \cdots S(1)	2.986	149.71
C(31)–H(31a) \cdots S(1)	3.028	163.98
C(41)–H(41a) \cdots S(2)	2.953	168.57
C(34)–H(34b) \cdots S(3)	3.024	126.27
C(22)–H(22b) \cdots S(4)	2.856	148.30
C(11)–H(11b) \cdots S(5)	2.965	173.94
S(6) \cdots S(6)*	3.473	–

only significant nonplanar deviations in the complex are those of the remaining sulphur atoms S(5) and S(6) that deviate from the average plane by 0.14 and 0.31 \AA , respectively.

The crystal structure of **4** is made up of zig-zag chains of $[\text{Au}(\text{dtpdt})_2]$ along the c axis; these are connected by short (3.473 \AA) S(6) \cdots S(6)* contacts (Figure 4).

The channels between the zig-zag chains of the anions are occupied by tetra-*n*-butyl ammonium (TBA) cations that are

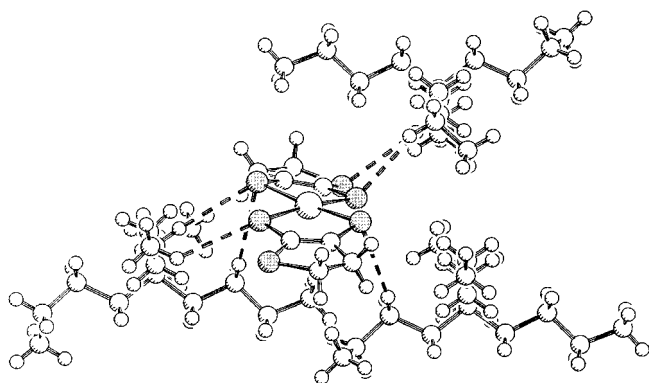


Figure 2. View of the $[\text{Au}(\text{dtpdt})]^-$ anion in **4** showing its distortion and the $\text{C}-\text{H}\cdots\text{S}$ bonds with surrounding cations.

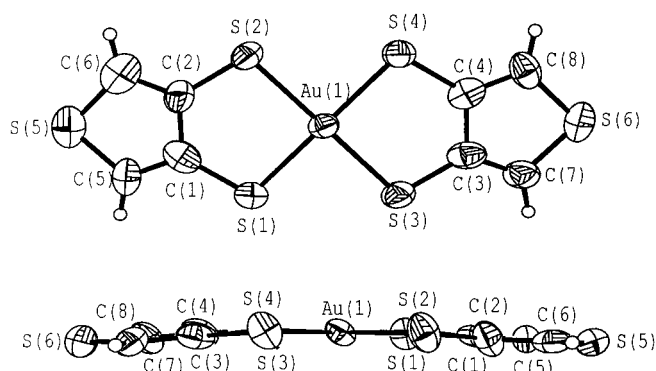


Figure 3. ORTEP views and atomic numbering scheme of $[\text{Au}(\text{tpdt})_2]^-$ (**6**) with thermal ellipsoids at 40% probability level.

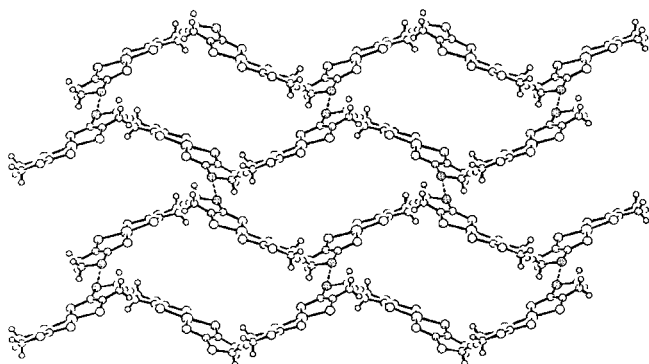


Figure 4. Zigzag chains of $[\text{Au}(\text{dtpdt})]^-$ anions in **4** emphasizing the short $\text{S}(6)\cdots\text{S}(6)^*$ contacts.

strongly held by a charge-assisted $\text{C}-\text{H}^{\delta+}\cdots\text{S}^{\delta-}$ hydrogen-bond system with $\text{H}\cdots\text{S}$ distances that range from 2.856 to 3.028 Å (see Table 2). It should be noted that, certainly due to these hydrogen bonds, the packing of the complex in the crystal structure of compound **4** (Figure 5) does not show any orientational disorder as was observed in the corresponding donor BET-TTF.^[16a, 17]

The structure of **6** consists of alternating layers of tetrabutylammonium cations and $[\text{Au}(\text{tpdt})_2]$ anions which are parallel to the ab plane (Figure 6).

The anion layers are composed of parallel chains of gold dithiolate units connected by short (3.470 Å) contacts be-

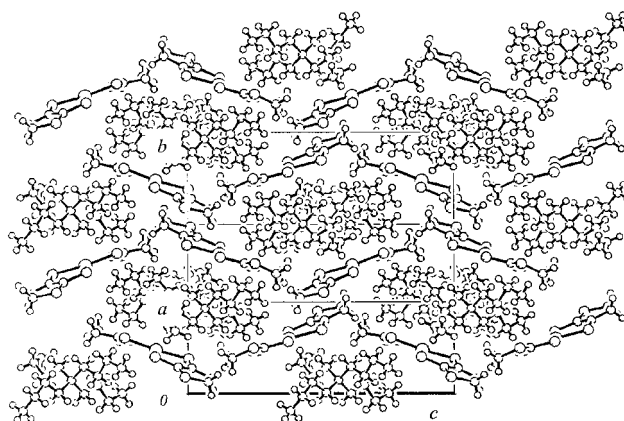


Figure 5. View of the crystal structure of **4** with the cations between the anion chains.

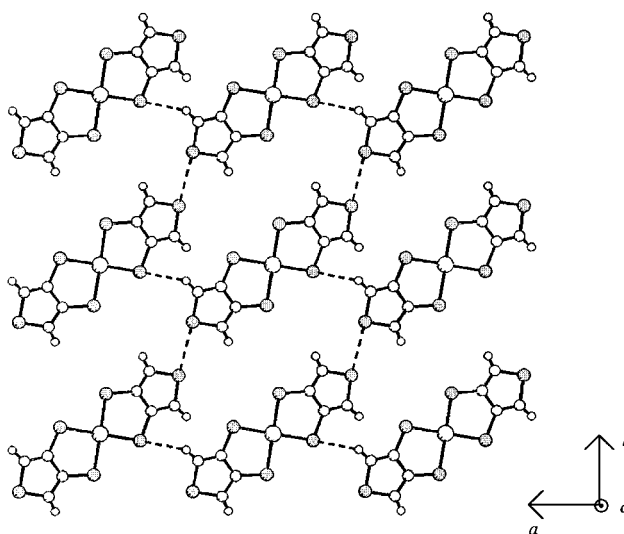


Figure 6. Anion layer in **6** emphasizing the short $\text{S}(5)\cdots\text{S}(6)^*$ contacts and the $\text{C}(7)-\text{H}(7)\cdots\text{S}(2)$ hydrogen bonds responsible for the two-dimensional network.

tween the terminal sulphur atoms $\text{S}(5)\cdots\text{S}(6)^*$. These chains are connected in layers by strong $\text{C}(7)-\text{H}(7)\cdots\text{S}(2)$ hydrogen bonds (Figure 7, Table 3).

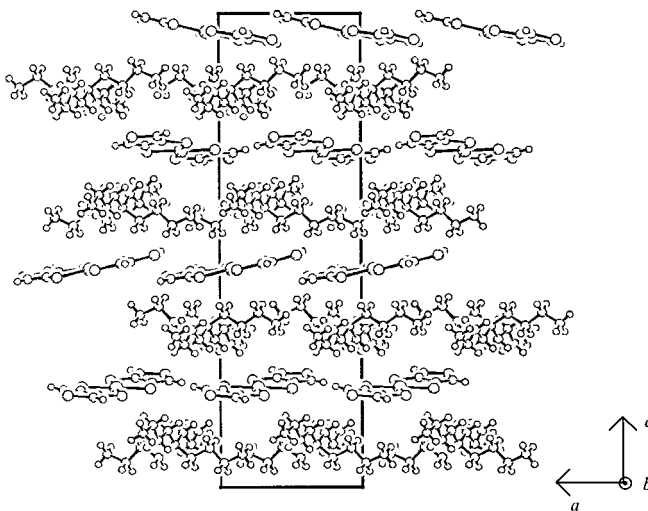
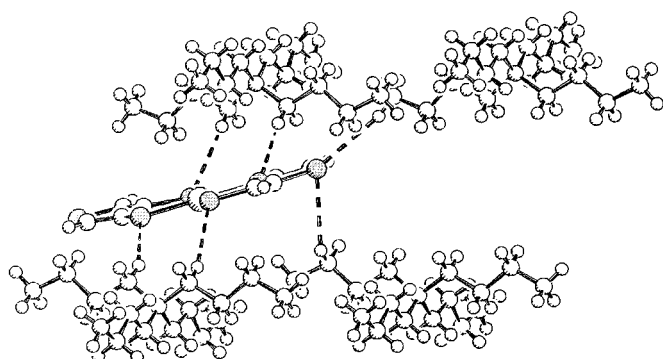


Figure 7. View of the crystal structure of **6** along the b axis.

Table 3. Hydrogen bonds and short contacts in the crystal structure of compound **6**.

	<i>d</i> [Å]	Angle [°]
C(21)–H(21b) ⋯ S(1)	2.918	159.42
C(31)–H(31b) ⋯ S(2)	2.982	171.68
C(7)–H(7) ⋯ S(2)	2.930	131.91
C(41)–H(41a) ⋯ S(3)	3.020	157.75
C(11)–H(11b) ⋯ S(4)	3.049	153.99
C(43)–H(43b) ⋯ S(5)	3.031	121.28
C(14)–H(14a) ⋯ S(5)	3.042	163.04
S(5) ⋯ S(6)*	3.470	–

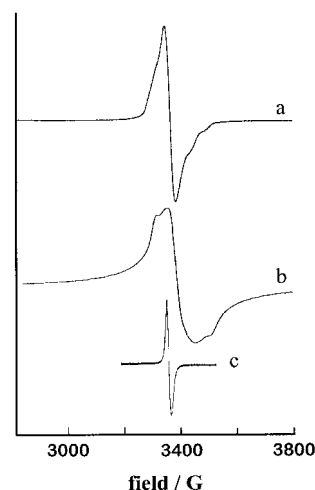
Adjacent anionic layers exhibit a chain orientation that is perpendicular to one another due to the 4_3 screw axis along *c*. Hydrogen bonds that involve all internal coordinating sulphur atoms and S(5) in the dithiolate as well as the inner ethylenic groups of *n*-Bu₄N from the adjacent cationic layers on both sides were observed to exist (Figure 8).

Figure 8. Hydrogen bonds between the anion of **6** and neighbouring cations.

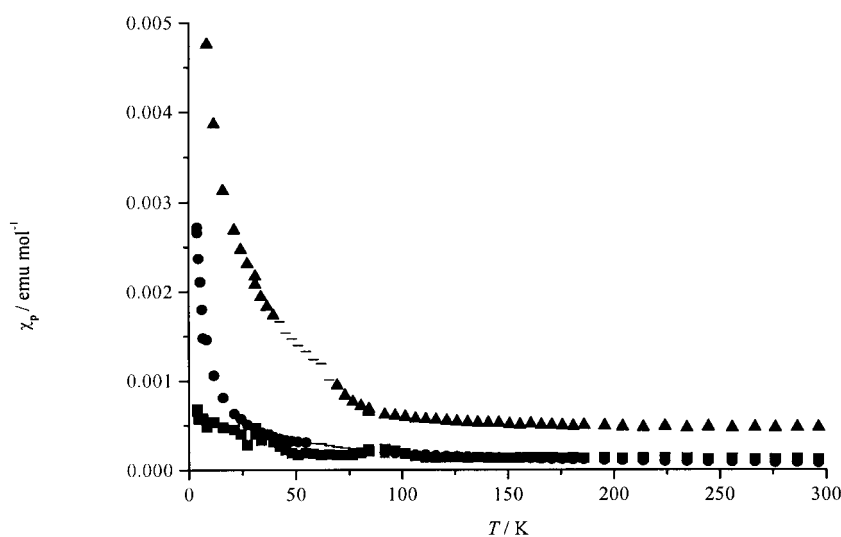
It is worth noting that the two-dimensional structure of the anionic layer observed in compound **6** no longer exists in compound **4**, due to the change of the position of the sulphur atom in the thiophenic ring.

As was expected for gold(III) with a d^8 configuration in a square-planar coordination, the anionic complexes are diamagnetic. However, the oxidised species are paramagnetic. Powder samples of the neutral complexes **7** and **8** have EPR signals; for compound **7** these are visible only below 200 K. At 10 K, the spectra of these compounds show a structure that corresponds to a rhombic anisotropy with the values of $g_1 = 1.942$, $g_2 = 2.008$, $g_3 = 2.055$ for [Au(α -tpdt)₂] (**8**) and $g_1 = 1.973$, $g_2 = 2.013$, $g_3 = 2.044$ for [Au(dtpdt)₂] (**7**). The spectrum of *n*-Bu₄N[$\{$ Au(tpdt)₂ $\}_{n-2}$] (**9**) also shows an EPR signal, already visible at room temperature at $g = 2.010$ with no resolved structure and a linewidth

of 13.5 G; this indicates either the coexistence of Au^{IV} and Au^{III} or an intermediate Au^{III-IV} oxidation state. This linewidth at low temperatures is much narrower than those of other neutral complexes (40 G and 103 G for **8** and **7**, respectively), thus the existence of more isolated Au^{IV} species diluted in Au^{III} species is supported (Figure 9). This is further supported by visible-NIR spectra, which contain no indications of the charge-transfer bands that are typical of mixed valence species.

Figure 9. EPR spectra at 10 K of polycrystalline samples of a) [Au(α -tpdt)₂] (**8**), b) [Au(dtpdt)₂] (**7**) and c) *n*-Bu₄N[$\{$ Au(tpdt)₂ $\}_{n-2}$] (**9**).

Static magnetic susceptibility measurements of these three compounds in the temperature range 4–300 K (Figure 10) confirm the paramagnetic behaviour of these compounds. However, the paramagnetic susceptibility, calculated from the raw measurements after correction for the diamagnetism estimated from tabulated Pascal constants, is rather small; 2.0×10^{-4} , 2.5×10^{-4} and 5×10^{-4} emu mol⁻¹ at room temperature for compounds **7**, **8** and **9**, respectively. Particularly in the case of compound **8**, the small paramagnetic susceptibility is almost independent of the temperature over a wide

Figure 10. Temperature dependence of the paramagnetic susceptibility, χ_p , of compounds **7** (●), **8** (■) and **9** (▲).

temperature range, which for this compound extends down to 10 K with a negligible Curie tail. This behaviour is reminiscent of the Pauli paramagnetic susceptibility of metallic systems. On the other hand, the larger value of susceptibility for compound **9** as well as the temperature dependent behaviour also supports the existence of isolated Au^{IV} species in this compound (Figure 10).

The insolubility of these neutral compounds makes the preparation of crystals of sufficient size very difficult and prevented any single-crystal transport measurements from being carried out with these compounds. However, four-probe electrical conductivity measurements were performed in compressed powder pellets. These measurements of the polycrystalline samples were expected to be dominated by interparticle resistance and possibly be further enhanced by anisotropy effects. Based on empirical evidence from measurements in many different molecular conductors, the electrical conductivity in powder samples is expected to be typically between 10^{-2} and 10^{-3} times smaller than that observed in single crystals along their most conductive axis.

Electrical conductivity data at room temperature in these powder samples have values of the order 10^{-9} Scm^{-1} for compound **9**, $3.3 \times 10^{-6} \text{ Scm}^{-1}$ for **7**, and 6 Scm^{-1} for **8**. Taking into account the usual difference between single-crystal and powder data, this last value is exceptionally large and probably places compound **8** among the molecular metals with the highest electrical conductivity. The temperature-dependent electrical conductivity, $\sigma(T)$, data of this compound (Figure 11) decrease upon cooling as is expected for a

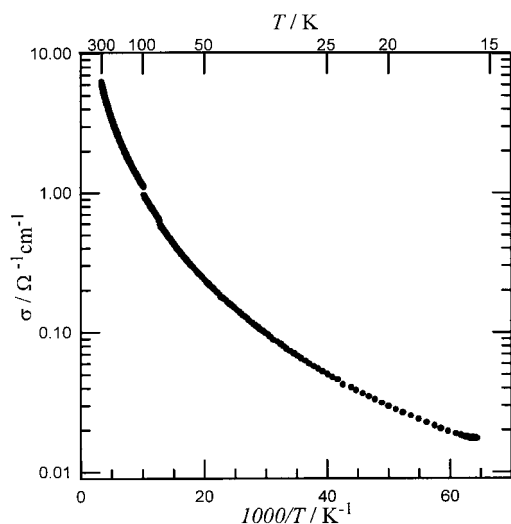


Figure 11. Electrical conductivity, σ , of a polycrystalline sample of **8** as a function of temperature.

polycrystalline sample due to the interparticle resistance effects. The temperature dependence of the electrical conductivity does not present a simple activation energy; the values of $d\ln\sigma/d(1/T)$ are quite small and range from 19.5 meV at room temperature to 3.5 meV at 20 K, a typical behaviour for a mixture of hopping and interparticle-tunneling processes.

At variance with electrical conductivity, thermopower, a zero-electrical-current measurement, probes the intrinsic properties of the material, because it is not so sensitive to the intercrystalline boundaries. Thermopower data in a compressed pellet of compound **8** (Figure 12) have very small

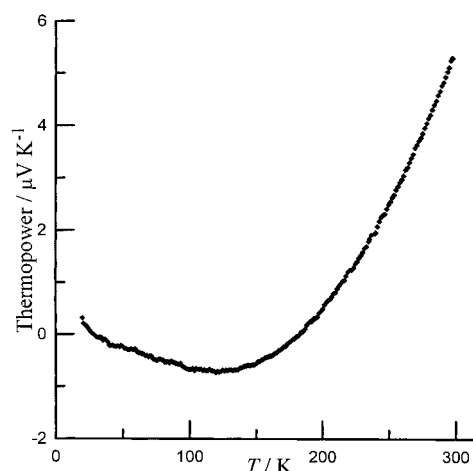


Figure 12. Absolute thermoelectric power of a polycrystalline sample of **8** as a function of temperature.

values over the entire temperature range of 15–300 K, with a maximum of $5.5 \mu\text{V K}^{-1}$ at room temperature. Thermopower values decrease upon cooling and cross zero at approximately 190 K, and reach a minimum of $-0.6 \mu\text{V K}^{-1}$ at approximately 120 K. Below this temperature, the values decrease almost linearly with decreasing temperature and approach zero. Not only is the small magnitude of the thermopower data typical of a metal, but its temperature dependence, approaching zero upon cooling at lower temperatures with a linear behaviour between 100 K and 20 K, is also clearly indicative of a system with the Fermi level lying in a continuum of states.

Despite the absence of single-crystal data, the magnetic susceptibility, electrical conductivity and thermoelectric power data indicate that compound **8** is a metal in the range of 15–300 K. To the best of our knowledge, this is the first molecular material based on a neutral species that has high electrical conductivity and metallic properties. A renewed interest in the synthesis of molecular conductors that are based on neutral species has recently made progress. The few successful examples of conductors based on neutral species^[20] are semiconductors and the highest conductivity reported was obtained for a single crystal of a Ni complex^[20b] that exhibited a conductivity of 7 Scm^{-1} at room temperature, approximately the same value as was observed in a powder compacted sample of compound **8**. To date, all known metals based on molecules are charge-transfer compounds for which the electrical conductivity is due to partially filled bands that originate from partially oxidised donors and/or partially reduced acceptors.

In the absence of a crystal structure, it is difficult to speculate further about the electronic structure and the origin of the metallic properties that were observed in compound **8**. However, most of the metallic properties of this compound are probably due to an energy overlap of the bands that

originate from the nonmixing of the fully occupied HOMO and singly occupied molecular SOMO orbital and thus lead to a semimetal with nonintegral band filling.

Conclusion

In conclusion, we have prepared and characterised new gold(III) complexes that are based on thiophenedithiolate ligands. These sulphur-rich ligands can stabilise higher oxidation states of the complexes; the air-stable neutral paramagnetic species was isolated for $[\text{Au}(\alpha\text{-tpdt})_2]$ (**8**) and $[\text{Au}(\text{dtpdt})_2]$ (**7**), for the tpdt ligand only $n\text{-Bu}_4\text{N}-[\text{Au}(\text{tpdt})_2]_{n-2}$ (**9**) could be obtained. The neutral complex $[\text{Au}(\alpha\text{-tpdt})_2]$ (**8**), characterised as a polycrystalline sample, exhibits the properties typical of a metal and was observed for the first time in a molecular system based on a neutral species.

These gold bis(thiophenedithiolate) complexes open the way to the synthesis of a larger family of new complexes based on different transition metals which will be reported in subsequent papers. These complexes provide useful building blocks with high potential for preparing interesting and novel conducting and magnetic materials.

Experimental Section

General: All procedures were performed under the exclusion of air in nitrogen or argon (CV) unless stated otherwise. All solvents were purified following standard procedures. Thieno[3,4-d]-1,3-dithiol-2-thione (**3**) was prepared by an analogous procedure to that in ref. [16a]. 5,6-Dihydrothieno[2,3-d]-1,3-dithiol-2-one (**1**) was synthesised as previously described.^[17] Other chemicals were commercially obtained and used without further purification. Column chromatography was carried out using silica gel (0.063–0.2 mm) from SDS. UV/Vis spectra were recorded on a Cary 5 G spectrophotometer (Varian). IR spectra were obtained on a Perkin Elmer 577 spectrophotometer. ¹H NMR spectra were recorded on a Bruker Aspect 3000 (300 MHz for ¹H) and CD₂Cl₂ was used as the solvent, TMS was the internal reference. MALDI mass spectra were obtained in time-of-flight negative linear mode on a Kratos Kompactaldi 2K probe (KRATOS Analytical) that was operated with pulsed extraction of the ions. Cyclic voltammetry data were obtained using a EG&G PAR 263A potentiostat galvanostat with a cell equipped with a double KCl (3M) bridge. The measurements were performed at room temperature in dichloromethane that contained $n\text{-Bu}_4\text{PF}_6$ as the supporting electrolyte, with a scan rate of 100 mV s⁻¹, platinum wire working- and counter-electrodes and a Ag/AgCl reference electrode.

Table 5, 6-Thieno[2,3-d]-1,3-dithiol-2-one (2): A solution of 5,6-dihydrothieno[2,3-d]-1,3-dithiol-2-one (**1**, 0.686 g, 3.9 mmol) and DDQ (1.869 g, 8.2 mmol) in toluene (25 mL) was stirred for 3 h at 120 °C. After removal of the solvent by evaporation, the product was purified by column chromatography by using $n\text{-hexane/ethyl acetate}$ (10:1) as eluent ($R_f=0.62$). Crystallisation in hexanes afforded the pure product as white needles in quantitative yield. M.p: 79.5 °C; FT IR (KBr): $\tilde{\nu}=370$ (w), 400 (m), 455 (m), 695 (s), 775 (s), 840 (m), 911 (m), 1080 (w), 1060 (w), 1340 (w), 1370 (w), 1608 (s), 1640 (s), 1685 (m, C=O), 3070 cm⁻¹ (w, C–H arom); elemental analysis calcd (%) for C₅H₄OS₂: C 34.46, H 1.16, S 55.20; found C 34.10, H 1.01, S 55.10; ¹H NMR (CD₂Cl₂): $\delta=7.87$ (d, 1H), 7.42 (d, 1H); MS: m/z (%): 173.90 (100) [M]⁻.

Table Tetrabutylammonium salt of gold(III) bis(2,3-dihydro-5,6-thiophenedithiolate), $n\text{-Bu}_4\text{N}[\text{Au}(\text{dtpdt})_2]$ (4): Ligand **1** (100 mg, 5.7×10^{-4} mol) was added to a solution of potassium methoxide in methanol (10 mL, 2M) while stirring. The resulting yellow solution was filtered and added to a solution of potassium tetrachloroaurate (107.7 mg, 2.9×10^{-4} mol) in methanol (2 mL), which became a green mixture. The inorganic precipitate was removed by filtration and the liquor added to a solution of tetrabutylam-

monium bromide (91.9 mg, 2.9×10^{-4} mol) in acetone (1 mL); a yellow-green precipitate was formed. The solid was filtered and recrystallised in acetone/isopropyl alcohol 3 : 1 to afford green-yellow needles. Stirring was maintained in all steps only until no visible modification was observed. The best crystals, which were suitable for X-ray crystal measurements, were obtained from crystallisation in acetonitrile. Yield: 50%; m.p. 95.2–96.2 °C; FT IR (KBr): $\tilde{\nu}=350$ (m, Au–S), 730 (m, CH₂–S–CH₂), 960 (m), 1370 (m), 1430(m), 1450 (m), 1480 (m), 1560 (w), 2800–2950 cm⁻¹ (br, C–H aliph); elemental analysis calcd (%) for C₂₄H₄₄NS₆Au: C 39.17, H 6.03, N 1.90, S 26.20; found C 39.07, H 6.52, N 1.99, S 26.07; UV/Vis (CH₃CN): $\lambda_{\text{max}}=585$, 882 nm; MS: m/z (%): 493.8 (100) [M]⁻.

Gold(IV) 2,3-dihydro-5,6-thiophenedithiolate, $[\text{Au}(\text{dtpdt})_2]$ (7): A solution of iodine (15.4 mg, 6.15×10^{-2} mmol) in acetone (2 mL) was added dropwise to a solution of **4** (89.5 mg, 1.23×10^{-1} mmol) in acetone (2 mL). The resulting dark precipitate was isolated by centrifugation, washed with acetone and dried in vacuo. Yield 28%; FT IR(KBr): $\tilde{\nu}=1070$ (m), 1325 (m), 1400 (w), 1600 cm⁻¹ (w); elemental analysis calcd (%) for C₈H₈S₆Au: C 19.47, H 1.63, S 38.98; found C 19.42, H 1.58, S 37.98; EPR: $g_1=1.973$, $g_2=2.013$, $g_3=2.044$; MS: m/z (%): 493.2 (100) [M]⁻.

Tetrabutylammonium salt of gold(III) bis(2,3-thiophenedithiolate), $n\text{-Bu}_4\text{N}[\text{Au}(\alpha\text{-tpdt})_2]$ (5): The compound was prepared by using the same method described for **4**. The initial reactant was 5,6-thieno[2,3-d]-1,3-dithiol-2-one (**2**). The product was obtained as red plates. Yield 68%; m.p. 140.8–141.4 °C; IR(KBr): $\tilde{\nu}=345$ (m, Au–S), 595 (s), 680 (s), 690 (s), 870(s), 1370 (s), 1390(s), 1475(s), 2800–2950 (br, C–H aliph), 3000–3100 cm⁻¹ (br, C–H arom); elemental analysis calcd (%) for C₂₄H₄₀NAuS₆: C 39.38, H 5.51, N 1.91, S 26.28; found C 39.77, H 4.67, N 1.97, S 26.45; UV/Vis (CH₃CN): $\lambda_{\text{max}}=540$, 857 nm; MS: m/z (%): 489 (100) [M]⁻.

Gold(IV) 2,3-thiophenedithiolate, $[\text{Au}(\alpha\text{-tpdt})_2]$ (8): By using starting material **5** and following the same procedure for **7**, the neutral species was obtained as a fine dark powder. Yield 74%; IR (KBr): no visible bands; elemental analysis calcd (%) for C₈H₈S₆Au: C 19.63, H 0.82, S 39.30; found C 19.07, H 0.85, S 39.02; EPR: $g_1=1.942$, $g_2=2.008$, $g_3=2.055$; MS: m/z (%): 489.2 (100) [M]⁻, 146.3 (49) [C₄H₉S₄]⁻.

Tetrabutylammonium salt of gold(III) bis(3,4-thiophenedithiolate), $n\text{-Bu}_4\text{N}[\text{Au}(\text{tpdt})_2]$ (6): The compound was prepared from thieno[3,4-d]-1,3-dithiol-2-thione (**3**) by following the same method described for **4**. The product was obtained as brown-yellow plates. Yield 53%; m.p. 198.5–198.7 °C. IR (KBr): $\tilde{\nu}=345$ (m, Au–S), 625 (m, C–S), 750 (s), 825 (s), 1305(s), 1470 (m), 1600(w), 2800–2950 (br, C–H aliph), 3000–3100 cm⁻¹ (br, C–H arom); UV/Vis (CH₃CN): $\lambda_{\text{max}}=434$, 645 nm; elemental analysis calcd (%) for C₂₄H₄₀NS₆Au: C 39.38, H 5.21, N 1.91, S 26.28; found C 39.24, H 5.46, N 1.89, S 26.74; MS: m/z (%): 489.0 (48) [M]⁻, 145.7 (100) [C₄H₉S₄]⁻.

Tetrabutylammonium salt of bis(gold(IV) bis(3,4-thiophenedithiolate), $n\text{-Bu}_4\text{N}[\text{Au}(\text{tpdt})_2]_{n-2}$ (9): Using starting material **6** and following the same procedure for **7**. Yield 51%; IR (KBr): $\tilde{\nu}=345$ (Au–S), 803 (w), 878 (w), 1127 (m), 1191 (m), 1282(s), 1359 (m), 1379 (s), 1459 (s), 1662 (br, w), 2870–2960 (s) (C–H aliph), 3087 cm⁻¹ (w) (C–H arom); elemental analysis calcd (%) for C₃₂H₄₄NS₁₂Au₂: C 31.47, H 3.63, N 1.15, S 31.50; found C 34.05, H 3.68, N 0.78, S 33.84; EPR: $g=2.010$; MS: m/z (%) 489.7 (100) [M]⁻.

EPR spectroscopy: EPR spectra in the temperature range of 4–300 K were obtained with an X-Band Bruker ESP 300E spectrometer equipped with a microwave bridge ER041XK, a rectangular cavity operating in T102 mode, a Bruker variable-temperature unit and an Oxford ESR-900 cryostat and a field controller ER 032M system. The modulation amplitude was kept significantly below the linewidth and the microwave power significantly below saturation.

Magnetic susceptibility measurements: Magnetic susceptibility measurements in the temperature range of 2–300 K were performed by using a longitudinal Faraday system (Oxford Instruments) with a 7 T superconducting magnet, under a magnetic field of 2 T and forward and reverse field gradients of 5 T m⁻¹. Polycrystalline samples (10–15 mg) were placed inside a previously calibrated thin-wall Teflon bucket. The force was measured with a microbalance (Sartorius S3D-V). Under these conditions, the magnetisation was found to be proportional to the applied magnetic field.

Electrical transport measurements: Electrical conductivity and thermoelectric power measurements of compressed pellets of the polycrystalline material were performed in the range 20–320 K, using a measurement cell attached to the cold stage of a closed cycle helium refrigerator. In the first

step, the thermopower was measured by using a slow ac (ca. 10^{-2} Hz) technique,^[21] by attaching two 60 μm diameter 99.99% pure Au wires (Goodfellow Metals), thermally anchored to two quartz reservoirs, with platinum paint (Demetron 308A) to the extremities of an elongated sample as in a previously described apparatus,^[22] controlled by a computer.^[23] The oscillating thermal gradient was kept below 1 K and was measured with a differential Au-0.05 at. % Fe versus chromel thermocouple. The sample temperature was measured by a previously calibrated thermocouple of the same type. The absolute thermoelectric power of the sample was obtained after correction for the absolute thermopower of the Au leads, by using the data of Huebner.^[24]

In the second step, electrical resistivity measurements of the same sample were performed using a four-probe technique. Two additional Au wires were placed on the sample in order to achieve a quadruple in-line contact configuration. Measurements were done by imposing a current of 1 μA at low frequency (77 Hz) through the sample and measuring the voltage drop with a lock-in amplifier.

X-ray crystallographic study: The crystal structures were solved by direct methods (programs SHELXS97 and SHELXL97^[27] for **4**, and SHELXS86^[28] and SHELXL93^[29] for **6**). Non-hydrogen atoms were refined anisotropically, hydrogen atoms were placed in idealised positions and allowed to be refined, while riding on the parent C atom. The absolute structure determination of complex **6** was done in space group $P4_3$, which gave the correct Flack parameter 0.07(6). Refinement in $P4_1$ space group was also tried, but observed to be the wrong one due to the high Flack parameter 0.91(6) and higher R_1 (0.0626) and wR_2 (0.1644) parameters. Further details of the crystal structure determination are given in Table 4. Graphical representations were prepared by using ORTEP3^[25] (Figures 1 and 3) and SCHAKAL 97.^[26] Crystallographic data (excluding structure factors) for the structures reported in this paper have been deposited in the Cambridge Crystallographic Data Centre as supplementary publication no. CCDC 138358 and CCDC 138357 for compounds $n\text{-Bu}_4\text{N}[\text{Au}(\text{tpdt})_2]$ (**6**) and $n\text{-Bu}_4\text{N}[\text{Au}(\text{dtpdt})_2]$ (**4**), respectively. Copies of

Table 4. Crystallographic data for compounds $n\text{-Bu}_4\text{N}[\text{Au}(\text{dtpdt})_2]$ (**4**) and $n\text{-Bu}_4\text{N}[\text{Au}(\text{tpdt})_2]$ (**6**).

	4	6
crystal size [mm]	$0.76 \times 0.38 \times 0.42$	$0.72 \times 0.18 \times 0.18$
crystal system	tetragonal	monoclinic
color/shape	yellow/needle	green/needle
space group	$P4_3$	$P2_1/c$
a [Å]	9.576(2)	9.583(2)
b [Å]		8.325(2)
c [Å]	32.549(4)	7.674(2)
β [°]		95.4(2)
V [Å ³]	2984.9(8)	3087.1(8)
formula	$\text{C}_{24}\text{H}_{40}\text{AuNS}_6$	$\text{C}_{24}\text{H}_{44}\text{AuNS}_6$
M_r	731.90	735.93
ρ_{calcd} [Mg m ⁻³]	1.629	1.583
μ [mm ⁻¹]	13.278	5.185
$F(000)$	1464	1480
diffractometer	Enraf Nonius Cad4	
radiation/ λ [Å]	$\text{Cu}_{K\alpha}/1.54150$	$\text{Mo}_{K\alpha}/0.71069$
T [K]	293(2)	293(2)
θ range [°]	4.62–66.90	1.61–24.97
index range (h,k,l)	$-11/1, 0/11, -38/1$	$-11/11, -1/21, -1/21$
scan type	ω -2 θ	ω -2 θ
data collection program	CAD4-software	
data reduction	process-MOLEN	
reflections collected	3544	6359
unique reflections	2814	5395
observed reflections [$I > 2\sigma(I)$]	2578	3793
absorption correction	psi-scans	
max/min. transmission	0.9977/0.8760	0.9995/0.9211
structure refinement	full-matrix least-squares	
goodness-of-fit on F^2	1.104	1.091
parameters	291	289
R (observed reflections)	0.0572	0.0440
wR_2 (observed reflections)	0.1543	0.0918

the data can be obtained free of charge upon application to the director of CCDC, 12 Union Road, Cambridge CB12 1EZ, UK (Fax: (+44) 1223-336-033, e-mail: deposit@ccdc.cam.ac.uk).

Acknowledgement

This work was partially supported by PRAXIS XXI (Portugal) under contracts 2/2.1/QUI/203/94 and 35452/99 and Direcció General de Enseñanza Superior (PB960862) and Generalitat de Catalunya (1998SGR-0106) (Spain). The collaboration between the team members of Sacavém and Barcelona was supported under the CSIC-ICCTI bilateral agreement. This work also benefited from COST action D14/0003/99.

- [1] a) *The Physics and Chemistry of Organic Superconductors* (Eds: G. Saito, S. Kagoshima), Springer, Berlin, **1990**; b) J. M. Williams, J. R. Ferraro, R. J. Thorn, K. D. Carlson, U. Geiser, H. H. Wang, A. M. Kini, M.-H. Whangbo, *Organic Superconductors, Including Fullerenes: Synthesis, Structure, Properties, and Theory*, Prentice-Hall, Englewood Cliffs, NJ, **1992**; c) *Organic Conductors; Fundamentals and Applications* (Ed: J.-P. Farges), Marcel-Dekker, New York, **1994**.
- [2] a) J. A. McLeverty, *Prog. Inorg. Chem.* **1968**, *10*, 29; b) D. Coucuvanis, *Prog. Inorg. Chem.* **1970**, *11*, 233; c) R. Eisenberg *Prog. Inorg. Chem.* **1970**, *12*, 295; d) L. Alcácer, H. Novais, *Extended Linear Chain Compounds, Vol. 3* (Ed.: J. S. Miller), Plenum, New York, **1983**, Chapter 6, p. 319; e) S. Alvarez, V. Ramon, R. Hoffman, *J. Am. Chem. Soc.* **1985**, *107*, 6253.
- [3] a) M. Almeida, V. Gama, R. T. Henriques, L. Alcácer, *Inorganic and Organometallic Polymers with Special Properties* (Ed.: R. M. Laine), Kluwer Academic, Dordrecht, **1992**, p. 163; b) V. Gama, R. T. Henriques, G. Bonfait, M. Almeida, S. Ravy, J. P. Pouget, L. Alcácer, *Mol. Cryst. Liq. Cryst.* **1993**, *234*, 171; c) M. Almeida, R. T. Henriques, *Organic Conductive Molecules and Polymers, Vol. 1* (Ed.: H. S. Nalwa), Wiley, Chichester, **1997**, Chapter 2, p. 87.
- [4] a) M. Ahamad, A. E. Underhill, *J. Chem. Soc. Chem. Commun* **1981**, 67; b) M. M. Ahamad, D. J. Turner, A. E. Hunderhill, C. S. Jacobsen, K. Mortensen, K. Carneiro, *Phys. Rev. B* **1984**, *29*, 4796.
- [5] P. Cassoux, L. Valade, *Inorganic Materials*, 2nd ed. (Eds.: D. W. Bruce, D. O'Hare), Wiley, Chichester, **1996**, p. 1.
- [6] P. Cassoux, J. S. Miller, *Chemistry of Advanced Materials* (Eds.: L. V. Interrante, M. J. Hampden-Smith), Wiley-VCH, New York, **1998**, p. 19.
- [7] J. H. Waters, H. B. Gray, *J. Am. Chem. Soc.* **1965**, *87*, 3534.
- [8] J. G. M. Van Rens, M. A. Vieggers, E. De Boer, *Chem. Phys. Lett* **1974**, *28*, 104.
- [9] R. L. Schlup, A. H. Maki, *Inorg. Chem* **1974**, *13*, 44.
- [10] J. Schultz, H. H. Wang, L. C. Soderholm, T. L. Sifter, J. M. Williams, K. Bechgaard, M. H. Whangbo, *Inorg. Chem.* **1987**, *26*, 3757.
- [11] G. Rindhorf, N. Thorup, T. Bjørnholm, K. Bechgaard, *Acta Crystallogr. Sect. C* **1990**, *46*, 1437.
- [12] N. C. Schioldt, T. Bjørnholm, K. Bechgaard, J. J. Neumeier, C. Allgeier, C. S. Jacobsen, N. Thorup, *Phys. Rev. B* **1996**, *53*, 17773.
- [13] E. B. Yagubskii, A. I. Kotov, E. E. Laukhina, A. A. Ignatev, L. I. Buravov, A. G. Khomenko, V. E. Shklover, S. S. Nagapetyan, Yu T. Struchkov, *Synth. Met.* **1991**, *42*, 215.
- [14] H. Fujiwara, E. Ojima, H. Kobayashi, T. Courcet, I. Malfant, P. Cassoux, *Eur. J. Inorg. Chem.* **1998**, 1631.
- [15] a) J. Tarrés, N. Santaló, M. Mas, E. Molins, J. Veciana, C. Rovira, S. Yang, H. Lee, D. O. Cowan, M.-L. Doublet, E. Canadell, *Chem. Mater.* **1995**, *7*, 1558; b) E. Coronado, L. Falvello, J. R. Galán-Mascarós, C. Giménez-Saiz, C. J. Gómez-García, V. Lauhkin, A. Pérez-Benítez, C. Rovira, J. Veciana, *Adv. Mater.* **1997**, *9*, 984; c) C. Rovira, J. Veciana, E. Ribera, J. Tarrés, E. Canadell, R. Rousseau, M. Mas, E. Molins, M. Almeida, R. T. Henriques, J. Morgado, J.-P. Schoeffel, J.-P. Pouget, *Angew. Chem.* **1997**, *109*, 2417; *Angew. Chem. Int. Ed. Engl.* **1997**, *36*, 21, 2324; d) C. Rovira, J. Veciana, E. Ribera, J. Tarrés, E. Canadell, R. Rousseau, M. Mas, E. Molins, M. Almeida, R. T. Henriques, J. Morgado, J.-P. Schoeffel, J.-P. Pouget, *Chem. Eur. J.* **1999**, *5*, 2025; for a review see e) C. Rovira in *Supramolecular Engineering of Synthetic*

- Metallic Materials* (Eds.: J. Veciana et al.), Kluwer Academic, **1999**, p. 377.
- [16] a) L. Y. Chiang, P. Shu, D. Holt, D. O. Cowan, *J. Org. Chem.* **1983**, *48*, 4713; b) C. Rovira, J. Veciana, N. Santaló, J. Tarrés, J. Cirujeda, E. Molins, J. Llorca, E. Espinoza, *J. Org. Chem.* **1994**, *59*, 3307.
- [17] A. Pérez-Benítez, J. Tarrés, E. Ribera, J. Veciana, C. Rovira, *Synthesis* **1999**, *4*, 577.
- [18] J.-C. Gabriel, I. Johansen, P. Batail, C. Coulon, *Acta Crystallogr. Sect. C* **1993**, *49*, 1052.
- [19] a) J. H. Enemark, J. A. Ibers, *Inorg. Chem.* **1968**, *7*, 2636; b) J. Tarres, M. Mas, E. Molins, J. Veciana, C. Rovira, J. Morgado, R. T. Henriques, M. Almeida, *J. Mater. Chem.* **1995**, *5*, 1653; c) N. G. Connelly, J. G. Crossley, A. G. Orpen, H. Salter, *J. Chem. Soc. Chem. Commun.* **1992**, 1564; d) J. C. Fitzmaurice, A. M. Z. Slawin, D. J. Williams, J. D. Woollins, *Polyhedron* **1990**, *9*, 1561; e) A. Domingos, R. T. Henriques, V. Gama, M. Almeida, A. L. Vieira, L. Alcácer, *Synth. Met.* **1988**, *27*, B411; f) P. Kuppusamy, N. Venkatalakshmi, P. T. Manoharan, *J. Crystallogr. Spectrosc. Res.* **1985**, *15*, 629; g) U. Kleinitz, R. Mattes, *Chem. Ber.* **1994**, *127*, 60; h) R. J. Staples, J. P. Fackler Junior, *Z. Kristallogr.* **1995**, *210*, 696.
- [20] a) X. Chi, M. E. Itkis, B. O. Patrick, T. M. Barclay, R. W. Reed, R. T. Oakley, A. W. Cordes, R. C. Haddon, *J. Am. Chem. Soc.* **1999**, *121*, 10395; b) A. Kobayashi, H. Tanaka, M. Kumasaki, H. Torii, B. Narymbetov, T. Adachi, *J. Am. Chem. Soc.* **1999**, *121*, 10763.
- [21] P. M. Chaikin and J. F. Kwak, *Rev. Sci. Instrum.* **1975**, *46*, 218.
- [22] M. Almeida, S. Oostra, L. Alcácer, *Phys. Rev. B* **1984**, *30*, 2839.
- [23] E. B. Lopes, INETI-Sacavem, internal report, **1991**.
- [24] R. P. Huebner, *Phys. Rev. A* **1964**, *135*, 1281.
- [25] P. McArdle, *J. Appl. Crystallogr.* **1995**, *28*, 65.
- [26] Egbert Keller, *Computer Program for the Graphic Representation of Molecular and Crystallographic Models*, Krystallographisches Institut der Universität Freiburg, Hebelstrasse 25, 79104 Freiburg, Germany.
- [27] G. M. Sheldrick, *SHELXL97: Program for the Refinement of Crystal Structures*, University of Göttingen, Germany, **1997**.
- [28] G. M. Sheldrick, *Acta Crystallogr. Sect. A* **1990**, *46*, 467.
- [29] G. M. Sheldrick, *SHELXL93: Program for the Refinement of Crystal Structures*, University of Göttingen, Germany, **1993**.

Received: July 5, 2000 [F2582]